
A Domain-Agnostic Scalable AI Safety Ensuring Framework

Beomjun Kim

Department of
Massachusetts Institute of Technology
Address
kimbj@mit.edu

Kangyeon Kim

School of Electrical Engineering
Korea Advanced Institute of Science and Technology
291 Daehak-ro, Yuseong-gu, Daejeon 34141, Republic of Korea
kky3528@kaist.ac.kr

Sunwoo Kim

Department of Statistics
Seoul National University
1 Gwanak-ro, Gwanak-gu, Seoul 08826, Republic of Korea
ksunw0209@snu.ac.kr

Heejin Ahn

School of Electrical Engineering
Korea Advanced Institute of Science and Technology
291 Daehak-ro, Yuseong-gu, Daejeon 34141, Republic of Korea
heejin.ahn@kaist.ac.kr

Abstract

Ensuring the safety of AI systems has recently emerged as a critical priority for real-world deployment, particularly in physical AI applications. Current approaches to AI safety typically address predefined domain-specific safety conditions, limiting their ability to generalize across contexts. We propose a novel AI safety framework that ensures AI systems comply with **any user-defined constraint**, with **any desired probability**, and across **various domains**.

In this framework, we combine an AI component (e.g., neural network) with an optimization problem to produce responses that minimize objectives while satisfying user-defined constraints with probabilities exceeding user-defined thresholds. For credibility assessment of the AI component, we propose *internal test data*, a supplementary set of safety-labeled data, and a *conservative testing* methodology that provides statistical validity of using internal test data. We also present an approximation method of a loss function and how to compute its gradient for training. We mathematically prove that probabilistic constraint satisfaction is guaranteed under specific, mild conditions and prove a scaling law between safety and the number of internal test data. We demonstrate our framework's effectiveness through experiments in diverse domains: demand prediction for production decision, safe reinforcement learning within the SafetyGym simulator, and guarding AI chatbot outputs. Through these experiments, we demonstrate that our method guarantees

safety for user-specified constraints, outperforms for **up to several order of magnitudes** existing methods in low safety threshold regions, and scales effectively with respect to the size of internal test data.

1 Introduction

As AI systems are increasingly deployed in safety-critical domains from healthcare to transportation, ensuring their safety has evolved from a technical preference to a societal imperative. While significant progress has been made García and Fernández [2015], Ribeiro et al. [2016], Mehrabi et al. [2021], current approaches typically address predetermined, domain-specific safety conditions, limiting their ability to generalize across contexts.

In this paper, we propose a framework that transforms any AI model into a system that ensures safety, defined as satisfying all user-specified constraints with user-specified probability thresholds. Our approach introduces an optimization problem that takes the AI model’s output and generates actions that optimize an objective function while satisfying constraints. A key innovation is the ability to handle *nondeterministic constraints* – those whose satisfaction cannot be deterministically evaluated, for example whether a text output is “harmless” in a chatbot example– by formulating them as chance constraints from stochastic control theory.

Nondeterministic constraints present a significant challenge for ensuring AI safety in real-world applications because most modern AI models are data-driven and thus inherently probabilistic in their outputs.

Chance constraints encode that the probability of constraint satisfaction remains above user-specified thresholds. To assess constraint satisfaction probabilities,

we introduce safety classification models and evaluate their credibility using **internal test data**– supplementary safety-labeled data. It can be portions of training data or replay buffers Mnih et al. [2015] in reinforcement learning. Since this internal test data influences training and creates statistical validity challenges, we propose **conservative testing**, a novel method that leverages the Lipschitz continuity property of AI models to ensure reliable overestimation of constraint satisfaction probabilities.

We mathematically prove that our approach guarantees probabilistic constraint satisfaction under specific conditions and prove that we can estimate the gradient of a loss function for training. Through experiments spanning production decision-making, reinforcement learning, and natural language generation, we demonstrate that our framework delivers provable safety while maintaining performance across diverse domains. Notably, our framework maintains meaningful performance even at extremely low safety thresholds, a capability that previous approaches have not been able to achieve. In the lowest thresholds levels, our method achieve up to 28, 412, 3.7 times safer with similar or superior performance. Moreover, we prove a scaling law between the quantity of internal test data and the safety guarantee. In particular, we prove that the required amount of internal test data is inversely proportional to the desired safety thresholds. To the best of our knowledge, this is the first scaling law proved in AI safety research. This result is also validated through experiments in reinforcement learning and natural language generation examples.

Our domain-agnostic, mathematically guaranteed safety framework with scaling properties lays the groundwork for deploying AI systems in safety-critical applications. Our contributions can be summarized as follows.

- We propose a domain-agnostic framework for safety-ensured AI that handles nondeterministic constraints through our novel internal test data and conservative testing methodology.
- We present how to train such safety-ensured AI in our framework by introducing an approximation of a loss function and computation of its gradient.
- We mathematically define and prove a scaling law for safety.
- We empirically validate the safety and performance.

2 Related Works

With the dramatic success of modern AI systems Amodei et al. [2016], AI safety is emerged as an important research area. AI safety research spans robustness to adversarial perturbations Goodfellow et al. [2015], safe reinforcement learning García and Fernández [2015], interpretability and explainability Ribeiro et al. [2016], fairness and bias mitigation Mehrabi et al. [2021], and aligning advanced systems with human values Amodei et al. [2016].

Moreover, since there is need for formally prove the safety of AI in some applications, there are effort to formally verify the behavior of neural networks. Reluplex introduces an SMT-based procedure that augments the classic Simplex algorithm with case-splitting on ReLU activations, enabling proofs or counter-examples for the behavior of feed-forward networks Katz et al. [2017]. Ehlers reformulates verification of piece-wise-linear networks as a mixed-integer linear program, showing that MILP solvers can give exact yes/no answers for safety properties on moderately sized networks while providing adversarial counter-examples when properties fail Ehlers [2017]. Huang et al. present a reachability analysis framework that propagates geometric over-approximations of each layer’s output to guarantee that all states reachable from a given input set satisfy a specified safety property Huang et al. [2017]. In this paper, we adopt the idea of reachability analysis in the design of conservative testing for the overestimation of posterior probability, assuming that the network is Lipchitz continuous.

On the other hand, there is a framework of decision-focused learning named **Predict-and-optimize**, in which machine learning models predict the input parameters of an optimization problem and are trained to maximize the quality of the resulting decisions rather than just predictive accuracy Donti et al. [2017], Kotary et al. [2021]. Key methods of this framework include differentiable optimization layers that embed solvers into neural networks Amos and Kolter [2017], decision-focused training that backpropagates through combinatorial optimizations Wilder et al. [2019], and surrogate loss functions that align prediction with the ultimate objective (e.g. the Smart “Predict-then-Optimize” loss) Elmachtoub and Grigas [2022]. Some approaches even treat the optimizer itself as part of the model—for example, a mixed-integer program can be incorporated as a network layer Ferber et al. [2020], or a linear surrogate can be learned for a complex combinatorial objective Ferber et al. [2023]. This framework also extends to black-box combinatorial solvers via specialized differentiation techniques Vlastelica et al. [2020]. We extend this framework to deal with a general continuous optimization problem without chance constraint in Section 4, 5 of Supplementary material part 1. Then, in the main text, we focus on re-generalizing it to handle nondeterministic constraints.

Reinforcement-learning safety has progressed from single-constraint tuning to formally grounded, shift-robust control. Constrained Policy Optimisation provides per-update guarantees Achiam et al. [2017]; temporal-logic shielding eliminates violations at run time Alshiekh et al. [2018]. Safety Gym benchmarked safe exploration Ray et al. [2019a], while risk-sensitive SAC Enders et al. [2024] and constraint-conditioned policies Yao et al. [2023] adapt quotas under distribution shifts.

3 Method

Our proposed framework combines AI models with an optimization problem to ensure that the outputs satisfy user-specified constraints. This approach generalizes the predict+optimize framework Amos and Kolter [2017] to handle nondeterministic safety constraints, which are inevitable due to inherent uncertainties in AI model predictions. To do that, we introduce two key innovations: internal test data for credibility assessment and conservative testing for robust probability estimation. We also present methods for computing gradients of the loss functions to enable end-to-end training.

3.1 Overall framework

Suppose an AI model f is given with trained weights $\mathbf{w}_0 \in \mathbb{R}^{n_w^1}$, which takes measurement $\mathbf{y} \in \mathcal{Y} \subset \mathbb{R}^{n_y}$ of the unknown environment state $\mathbf{s} \in \mathcal{S} \subset \mathbb{R}^{n_{s1}} \times \mathbb{Z}^{n_{s2}}$ as input and procudes a continuous vector $f(\mathbf{y}; \mathbf{w}_0) \in \mathbb{R}^{n_f}$ as the output. The output $f(\mathbf{y}; \mathbf{w}_0)$ is post-processed to make a continuous and discrete prediction (or action) $\mathbf{u} \in \mathcal{U} \subset \mathbb{R}^{n_{u1}} \times \mathbb{Z}^{n_{u2}}$. We say the AI model

¹ \mathbb{R}^{n_\star} is the space of n_\star -dimensional real vectors, and \mathbb{Z}^{n_\star} is the space of n_\star -dimensional integer vectors.

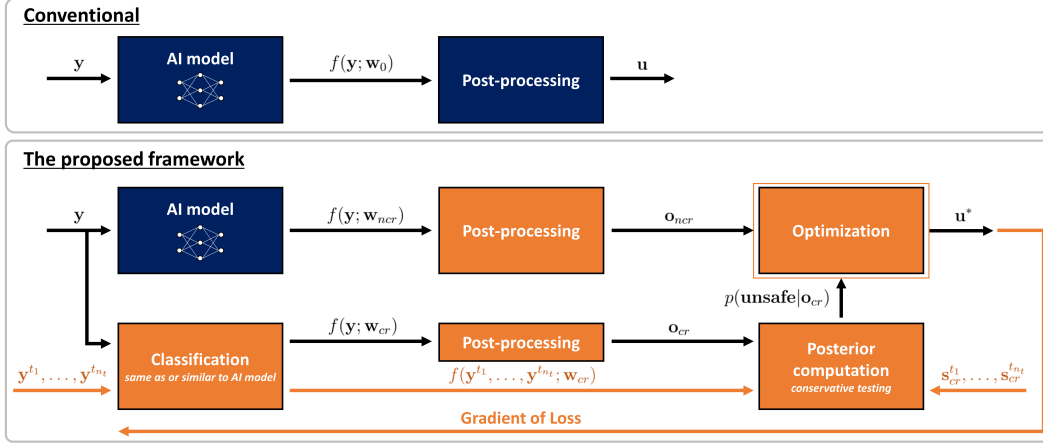


Figure 1: Our proposed framework

guarantees safety if all its actions satisfy user-specified constraints $c_i(\mathbf{u}; \mathbf{s}, \mathbf{r}) \geq 0$ for $i = 1, \dots, n_c$ under the environment state \mathbf{s} and user-given parameters $\mathbf{r} \in \mathbb{R}^{n_r}$.

Because an AI model cannot guarantee safety in general due to its data-driven nature, we introduce an optimization component that forces actions to satisfy safety constraints while maintaining high performance. The goal is to minimize an objective $J(\mathbf{u}; \mathbf{s}, \mathbf{r})$ while satisfying constraints $\mathbf{c}(\mathbf{u}; \mathbf{s}, \mathbf{r}) \geq 0$ where $J: \mathcal{U} \rightarrow \mathbb{R}$ and $\mathbf{c}: \mathcal{U} \rightarrow \mathbb{R}^{n_c}$ are specified by users and thus known. However, since we do not exactly know the environment state \mathbf{s} , we cannot guarantee constraint satisfaction deterministically.

We formulate such nondeterministic constraints as chance constraints, bounding the probability of violation as follows:

$$Pr(c_i(\mathbf{u}; \mathbf{s}, \mathbf{r}) < 0) \leq r_{t,i}, \quad i = 1, \dots, n_c, \quad (1)$$

where $r_{t,i} \in \mathbb{R}$ is a user-given threshold and n_c is the number of constraints.

Depending on the constraints, we divide the environment state into two parts $\mathbf{s} = (\mathbf{s}_{cr}, \mathbf{s}_{ncr})$ where $\mathbf{s}_{cr} \in \mathcal{S}_{cr}$ is the necessary part of the environment state to determine the safety constraints \mathbf{c} and $\mathbf{s}_{ncr} \in \mathcal{S}_{ncr}$ is the remainder. Since the environment state \mathbf{s} is an unobserved variable, we need to estimate the environment state using the measurement \mathbf{y} . To obtain its estimate $\mathbf{o} \in \mathcal{O}$, we introduce two AI models, one to produce \mathbf{o}_{cr} that estimates \mathbf{s}_{cr} and the other to produce \mathbf{o}_{ncr} that estimates \mathbf{s}_{ncr} . In practice, we use the same structure f as the given AI model or a reduced variant thereof, but with different weights $\mathbf{w}_{cr} \in \mathbb{R}^{n_w}$ and $\mathbf{w}_{ncr} \in \mathbb{R}^{n_w}$, and post-process the outputs to generate the estimate \mathbf{o}_{cr} and \mathbf{o}_{ncr} , respectively. Specifically, \mathbf{o}_{cr} is the post-processed result of $f(\mathbf{y}; \mathbf{w}_{cr})$, and \mathbf{o}_{ncr} is the post-processed result of $f(\mathbf{y}; \mathbf{w}_{ncr})$. For simplicity, we assume \mathbf{s}_{cr} and \mathbf{o}_{cr} take discrete values—for example, classifying text as either ‘harmful’ or ‘harmless’ in a chatbot application. For this reason, we call $f(\mathbf{y}; \mathbf{w}_{cr})$ the safety classification model.

Now we reformulate the optimization problem using these estimates:

$$\min_{\mathbf{u} \in \mathcal{U}} \quad \bar{J}(\mathbf{u}; \mathbf{o}, \mathbf{r}) \quad (2a)$$

$$\text{subject to} \quad \bar{c}_i(\mathbf{u}; \mathbf{o}, \mathbf{r}) \geq 0, \quad i = 1, \dots, n_c. \quad (2b)$$

Here, the constraint \bar{c}_i is the chance constraint rewritten using the estimate \mathbf{o}_{cr} ,

$$\bar{c}_i(\mathbf{u}; \mathbf{o}, \mathbf{r}) \geq 0 \Leftrightarrow Pr(c_i(\mathbf{u}; \mathbf{s}_{cr}, \mathbf{r}) < 0 | \mathbf{o}_{cr}) \leq r_{t,i}, \quad i = 1, \dots, n_c. \quad (3)$$

This probability represents the posterior probability of constraint violation given the classification output \mathbf{o}_{cr} . The objective function \bar{J} is a function similar to J but written in terms of the estimate \mathbf{o} ; for example, $\bar{J}(\mathbf{u}; \mathbf{o}, \mathbf{r}) = E_{\mathbf{s}_{cr}}[J(\mathbf{u}; \mathbf{s}_{cr}, \mathbf{o}_{ncr}, \mathbf{r}) | \mathbf{o}_{cr}]$. To estimate the posterior probability in (3) in practice, we will introduce internal test data in the next subsection. Additional details on this formulation are provided in Section 2-3 of the supplementary material part 1.

Example 1. In a production decision example, the measurement \mathbf{y} is the historical demand data, the action \mathbf{u} is the production decision, and constraints \mathbf{c} can specify the ingredient limitations and prevent production of low-demand products.

Example 2. In a RL in SafetyGym example, the measurement \mathbf{y} is observation data obtained by (simulated) RIDAR and IMU, the action \mathbf{u} is the acceleration or rotation of the agent, and constraints \mathbf{c} can specify that the agent should not get in or collide to unsafe area.

Example 3. In a chatbot example, the measurement \mathbf{y} is the prompt given by the user, the action \mathbf{u} is the response of the chatbot, and constraints \mathbf{c} can specify that the response should be harmless.

3.2 Internal test and Conservative Testing

In this subsection, we present our method of computing the posterior probability $Pr(c_i(\mathbf{u}; \mathbf{s}_{cr}, \mathbf{r}) < 0 | \mathbf{o}_{cr})$ in (3). Since AI models (particularly neural networks) can be imperfectly trained, we cannot fully trust their outputs and must evaluate their credibility – specifically, the relationship between the constraint-related output \mathbf{o}_{cr} and environment state \mathbf{s}_{cr} . To address this challenge, we introduce internal test data: a safety-labeled dataset that helps assess model reliability. The constraint-related environment state \mathbf{s}_{cr} is provided as a safety label in this dataset, as constraints are determined once \mathbf{s}_{cr} is specified.

We denote the set of possible constraint-related environment states as $\mathcal{S}_{cr} = \{\bar{\mathbf{s}}_1, \dots, \bar{\mathbf{s}}_{n_{s_{cr}}}\}$ and the set of possible outputs as $\mathcal{O}_{cr} = \{\bar{\mathbf{o}}_1, \dots, \bar{\mathbf{o}}_{n_{o_{cr}}}\}$. Our internal test data consists of measurements $\mathbf{y}^{t_1}, \dots, \mathbf{y}^{t_{n_t}}$, each associated with environment state labels $\mathbf{s}_{cr}^{t_1}, \dots, \mathbf{s}_{cr}^{t_{n_t}}$, respectively.

To compute the posterior probability, we evaluate internal test data using the safety classification model $f(\mathbf{y}^{t_k}; \mathbf{w}_{cr})$ and perform post-processing (in this case, the argmax operation) to obtain $\mathbf{o}_{cr}^{t_k}$. Specifically, we compute the posterior $p(\mathbf{s}_{cr} = \bar{\mathbf{s}}_i | \mathbf{o}_{cr} = \bar{\mathbf{o}}_j)$ for each pair of (i, j) by applying Bayes’ rule Bayes and Price [1763] with a given prior $p(\mathbf{s}_{cr} = \bar{\mathbf{s}}_i)$ and the following likelihood estimated from internal test data

$$p(\mathbf{o}_{cr} = \bar{\mathbf{o}}_j | \mathbf{s}_{cr} = \bar{\mathbf{s}}_i) \approx \frac{\sum_{k=1}^{n_t} \mathbf{1}(\mathbf{s}_{cr}^{t_k}, \bar{\mathbf{s}}_i) \mathbf{1}(\mathbf{o}_{cr}^{t_k}, \bar{\mathbf{o}}_j)}{\sum_{k=1}^{n_t} \mathbf{1}(\mathbf{s}_{cr}^{t_k}, \bar{\mathbf{s}}_i)},$$

where $\mathbf{1}(x_1, x_2)$ is the indicator function that equals 1 when $x_1 = x_2$ and 0 otherwise. This estimation essentially counts how often output $\bar{\mathbf{o}}_j$ occurs when the environment state is $\bar{\mathbf{s}}_i$ in our internal test data.

A key challenge arises in this approach: we continuously train the AI model, and this training process incorporates gradients from the internal test data. Unlike traditional test data that remains separate from training, our internal test data influences the model through these gradients, thereby *leaking* into the model after the first epoch. Despite this leakage, we continue using the same data points in subsequent epochs, creating a statistical validity problem, that is, internal test data points are no longer independently and identically distributed samples from the input distribution.

To address this challenge of data leakage, we propose a novel method called **conservative testing**. This approach ensures we overestimate the posterior probability of constraint violations, provided that internal test data distribution is sufficiently close to the input distribution, without requiring it to be iid. The method leverages the Lipschitz continuity property of AI models, which ensures that similar inputs produce similar outputs with bounded differences. Then, the AI model output for the input data is similar to the AI model output to the internal test data with bounded differences, thus we can obtain conservative bound based on the output of internal test data.

In conservative testing, we consider a set of outputs within a radius of ξ centered at $f(\mathbf{y}^{t_k}; \mathbf{w}_{cr})$, defined as

$$\mathcal{B}(f(\mathbf{y}^{t_k}; \mathbf{w}_{cr})) := \{\phi : \|\phi - f(\mathbf{y}^{t_k}; \mathbf{w}_{cr})\| \leq \xi\}.$$

Then, we define two versions of indicator functions

$$\mathbf{1}^{+\xi}(f(\mathbf{y}^{t_k}; \mathbf{w}_{cr}), \bar{\mathbf{o}}_j) := \max_{\phi \in \mathcal{B}(f(\mathbf{y}^{t_k}; \mathbf{w}_{cr}))} \mathbf{1}(\text{argmax}(\phi), \bar{\mathbf{o}}_j), \quad (4)$$

$$\mathbf{1}^{-\xi}(f(\mathbf{y}^{t_k}; \mathbf{w}_{cr}), \bar{\mathbf{o}}_j) := \min_{\phi \in \mathcal{B}(f(\mathbf{y}^{t_k}; \mathbf{w}_{cr}))} \mathbf{1}(\text{argmax}(\phi), \bar{\mathbf{o}}_j) \quad (5)$$

where $\text{argmax}(\phi)$ is the post-processing operator for the safety classification model, returning the class corresponding to the maximum value in ϕ . The positive indicator $\mathbf{1}^{+\xi}$ equals 1 if any point in the ξ -ball would be classified as $\bar{\mathbf{o}}_j$, while the negative indicator $\mathbf{1}^{-\xi}$ equals 1 only if all points in the ξ -ball would be classified as $\bar{\mathbf{o}}_j$.

Using these indicator functions, we derive conservative upper and lower bounds on the conditional probability as

$$p^{\pm\xi}(\mathbf{o}_{cr} = \bar{\mathbf{o}}_j | \mathbf{s}_{cr} = \bar{\mathbf{s}}_i) := \frac{\sum_{k=1}^{n_t} \mathbf{1}(\mathbf{s}_{cr}^{t_k}, \bar{\mathbf{s}}_i) \mathbf{1}^{\pm\xi}(f(\mathbf{y}^{t_k}; \mathbf{w}_{cr}), \bar{\mathbf{o}}_j)}{\sum_{k=1}^{n_t} \mathbf{1}(\mathbf{s}_{cr}^{t_k}, \bar{\mathbf{s}}_i)}. \quad (6)$$

The validity of these bounds is formalized in the following theorem.

Theorem 1. *When the measurement space \mathcal{Y} has mild conditions, and ξ is sufficiently large, we can bound the conditional probability $p(\mathbf{o}_{cr} = \bar{\mathbf{o}}_j | \mathbf{s}_{cr} = \bar{\mathbf{s}}_i)$ as follows:*

$$p^{-\xi}(\mathbf{o}_{cr} = \bar{\mathbf{o}}_j | \mathbf{s}_{cr} = \bar{\mathbf{s}}_i) \leq p(\mathbf{o}_{cr} = \bar{\mathbf{o}}_j | \mathbf{s}_{cr} = \bar{\mathbf{s}}_i) \leq p^{+\xi}(\mathbf{o}_{cr} = \bar{\mathbf{o}}_j | \mathbf{s}_{cr} = \bar{\mathbf{s}}_i). \quad (7)$$

The formal conditions used in the theorem are provided in Section 4 of Supplementary material part 1, along with the proof of the theorem. The size of ξ depends on the quality of internal test data (we refer it as ζ -informativeness in Supplementary material) and the Lipschitz constant of AI models.

With the upper and lower bounds on the likelihood, we can compute the upper bound of the posterior probability $p(\mathbf{s}_{cr} = \bar{\mathbf{s}}_i | \mathbf{o}_{cr} = \bar{\mathbf{o}}_j)$ based on Bayes' rule as follows (Note that $p(\mathbf{s}_{cr} = \bar{\mathbf{s}}_i)$ is a user-given parameter (included in \mathbf{r})):

$$p^\xi(\mathbf{s}_{cr} = \bar{\mathbf{s}}_i | \mathbf{o}_{cr} = \bar{\mathbf{o}}_j) := \frac{p^{+\xi}(\mathbf{o}_{cr} = \bar{\mathbf{o}}_j | \mathbf{s}_{cr} = \bar{\mathbf{s}}_i) p(\mathbf{s}_{cr} = \bar{\mathbf{s}}_i)}{\sum_{k=1}^{N_e} p^{-\xi}(\mathbf{o}_{cr} = \bar{\mathbf{o}}_j | \mathbf{s}_{cr} = \bar{\mathbf{s}}_k) p(\mathbf{s}_{cr} = \bar{\mathbf{s}}_k)} \quad (8)$$

3.3 Approximate loss for training

For the AI models' output \mathbf{o} and the optimal solution \mathbf{u} of the optimization problem, we need to evaluate a loss function $L(\mathbf{u}, \mathbf{o}; \mathbf{s}, \mathbf{r})$ and compute its gradient with respect to the model weights \mathbf{w}_{cr} and $\mathbf{w}_{n_{cr}}$. However, this presents a challenge because the optimal action \mathbf{u} can be discontinuous with respect to \mathbf{o} . Additionally, when multiple optimal solutions exist, they may yield different loss values. These characteristics make the loss function discontinuous with respect to the model weights, preventing direct application of gradient-based training methods. To overcome this obstacle, we must develop a continuous approximation of the loss function.

We propose an approximate loss function that is applicable to general optimization problems with continuous objectives and constraints. This is an extension of prior work Vlastelica et al. [2020], which presents an approximate loss function for unconstrained problems with linear objective functions. We construct the approximate loss function for some parameters $\lambda \in \mathbb{R}$ and $\beta \in \mathbb{R}^{n_e}$ as follows:

$$\begin{aligned} \tilde{L}(\mathbf{o}; \mathbf{s}, \mathbf{r}, \beta, \lambda) := & \frac{1}{\lambda} \left(\min_{\mathbf{u} \in \mathcal{U}} (\lambda L(\mathbf{u}, \mathbf{o}; \mathbf{s}, \mathbf{r}) + \bar{J}(\mathbf{u}; \mathbf{o}, \mathbf{r}) - \beta^\top \min(\bar{\mathbf{c}}(\mathbf{u}; \mathbf{o}, \mathbf{r}), \mathbf{0})) \right. \\ & \left. - \min_{\mathbf{u} \in \mathcal{U}} (\bar{J}(\mathbf{u}; \mathbf{o}, \mathbf{r}) - \beta^\top \min(\bar{\mathbf{c}}(\mathbf{u}; \mathbf{o}, \mathbf{r}), \mathbf{0})) \right). \end{aligned} \quad (9)$$

The approximate loss function is the scaled difference between two optimal objectives, one incorporating the loss function L with weight λ and the other only with the optimization problem. For handling constraints, we incorporate them into the objective function using penalty terms β . This construction ensures that the approximate loss function \tilde{L} is continuous with respect to \mathbf{o} and approaches the true loss function L as λ becomes sufficiently small.

The following theorem guarantees that (9) is continuous with respect to \mathbf{o} and approaches to $L^*(\mathbf{o}; \mathbf{s}, \mathbf{r})$, which is defined as $L(\mathbf{u}^*, \mathbf{o}; \mathbf{s}, \mathbf{r})$ when \mathbf{u}^* is the optimal solution of (2).²

Theorem 2. *When $\bar{J}(\mathbf{u}; \mathbf{o}, \mathbf{r})$, $\bar{\mathbf{c}}(\mathbf{u}; \mathbf{o}, \mathbf{r})$, $L(\mathbf{u}, \mathbf{o}; \mathbf{s}, \mathbf{r})$ are continuous with respect to \mathbf{u} and \mathbf{o} ³, under mild conditions on \mathcal{U} ,*

$\tilde{L}(\mathbf{o}; \mathbf{s}, \mathbf{r}, \beta, \lambda)$ is continuous with respect to \mathbf{o} and approaches $L^(\mathbf{o}; \mathbf{s}, \mathbf{r})$ as β becomes large and λ small.*

We compute the gradient of $\tilde{L}(\mathbf{o}; \mathbf{s}, \mathbf{r}, \beta, \lambda)$ with respect to \mathbf{o} and then to \mathbf{w}_{cr} and $\mathbf{w}_{n_{cr}}$, and back-propagate it to train the AI models. The proof of Theorem 2 and details of gradient calculation are presented in Section 4, 5 of Supplementary material part 1, respectively.

²When there are multiple optimal solutions, we consider \mathbf{u}^* as an optimal solution that makes the smallest value of $L(\mathbf{u}^*, \mathbf{o}; \mathbf{s}, \mathbf{r})$.

³We consider continuities with respect to only the continuous part of \mathbf{o} .

4 Scaling Law

Traditional scaling laws in deep learning describe how computational requirements or performance metrics scale with the amount of training data. However, for AI safety systems, we must simultaneously optimize for performance while ensuring safety. This multi-objective nature makes defining scaling laws for AI safety non-trivial.

To address this challenge, we conceptualize the problem in terms of identifying a "safe set" within the action space \mathcal{U} . The primary goal of the safety component in our framework is to accurately classify actions as safe or unsafe. Once this classification is complete, the system can select the highest-performing action among those deemed safe.

We define our scaling law in terms of the data requirements for reliable safe set identification. Specifically, we quantify how many internal test data points are needed to bound both types of misclassification errors: classifying unsafe actions as safe (Type I error) and safe actions as unsafe (Type II error). The following theorem formalizes this relationship.

Theorem 3. *Let α be an upper bound of both the first-type error and second-type error probability. Under mild conditions of safe sets and assumption that the safety classification model is a universal approximator, the expected number N_{reqit} of required internal test data grows as*

$$N_{reqit} \leq A\alpha^{-n_y} \quad (10)$$

when A is the constant and n_y is the dimension of the measurement space \mathcal{Y} .

This theorem establishes an inverse power law relationship between the error bound α and the required number of internal test data points, with the exponent determined by the dimensionality of the measurement space. The formal definitions of conditions and the complete proof are provided in Section 6 of Supplementary material part 1.

5 Experiment results

In this section, we present results of our experiments. To show the domain-agnosticism, we validate our framework in three distinct domain: production planning with demand prediction, reinforcement learning in Safetygym, and natural language generation. In each domain, we employ traditional AI models (or sometimes reduced version for safety classification) as the neural network architecture of our framework, and use same networks for baselines, for fair comparison.

Our framework has an useful extension that helps to obtain high performance with different thresholds than threshold used in training. Please see Section 7 of Supplementary material part 1. We exploit this feature in the experiments. For all domains, we train our framework with only one threshold value and run validation with several thresholds, resulting in scatters plots describing the relationship of performance versus safety.

Due to the space limit, details for experiments is explained in Supplementary material part 2 rather than this section.

5.1 Production planning with demand prediction

As our first example, we apply our framework to production planning with demand prediction. In this scenario, a company must determine optimal production quantities $\mathbf{u} \in \mathbb{R}^4$ of four products based on uncertain future demand $\mathbf{s} \in \mathbb{R}^4$ to maximize revenue while satisfying material constraints and avoiding production when demand is too low.

Constraints: The system faces two types of constraints. First, deterministic material limitations are formulated as $A\mathbf{u} + |\mathbf{u}| \leq \mathbf{b}$, where A and \mathbf{b} are fixed matrices and vectors representing material consumption rates and availability limits. The element-wise absolute value $|\mathbf{u}|$ creates robustness against uncertainties in the consumption rates, handling worst-case scenarios where actual consumption might deviate from nominal values A . This robust formulation can be expressed as a second-order cone constraint. Second, we introduce nondeterministic constraints: when the demand for the i th product is too low ($s_i < 3$, where demand is normalized to $[0, 10]$), production should cease ($u_i = 0$) due to inefficient distribution networks. We limit the probability of violating this constraint below a user-specified threshold r_t .

AI model: For the AI model, we use a LSTM architecture to process historical demand data \mathbf{y} from the previous 24 time steps and predict demand estimate $\mathbf{o}_{ncr} = (o_{ncr,1}, \dots, o_{ncr,4})$ of the products. For the safety classification model, we use the same LSTM architecture to generate $\mathbf{o}_{cr} = (o_{cr,1}, \dots, o_{cr,4}) \in \{0, 1\}^4$ where $o_{cr,i} = 1$ indicates the prediction that $s_i < 3$.

Internal test data: We use a quarter of our data for training data, another quarter as internal test data used in training, another quarter as data for validation, and the other quarter as the internal test data for validation. We then apply conservative testing to compute reliable upper bounds on the posterior probability of low demand given the classifier outputs.

Optimization: Production quantities are set to zero when this bound exceeds the user-specified threshold r_t , and otherwise optimized to maximize revenue. Considering that market price is influenced by supply and demand, the revenue is formulated as $\sum_{i=1}^4 (p_i - k_i(u_i - s_i)) \cdot u_i$ where standard price (p_1, p_2, p_3, p_4) and price sensitivity parameters (k_1, k_2, k_3, k_4) are given constants.

Results: Figure 2 illustrates the performance versus constraint violation trade-off. The x -axis shows the percentage of cases where production continues despite low demand (constraint violation), while the y -axis shows total revenue across 8,760 time steps. Note that constraint violations only occur for the nondeterministic constraint regarding low demand, as our approach guarantees perfect satisfaction of deterministic constraints. In this experiment, we use $r_t = 0.001$ for training and $0.001 - 1.0$ for validation. The results demonstrate that our method achieves significantly higher revenue than baseline approaches, particularly when strict constraint satisfaction is required (low violation percentage). We compare against “MeanVar” (production decisions based on mean and variance of historical demand), “Twostage” (independently learned demand prediction), and “End-to-End” (direct learning from historical data to production decisions). Since existing predict-and-optimize methods cannot handle second-order cone constraints, these alternative approaches represent the best available baselines. This example demonstrates our framework’s ability to handle both deterministic and nondeterministic constraints while achieving superior performance in real-world optimization scenarios.

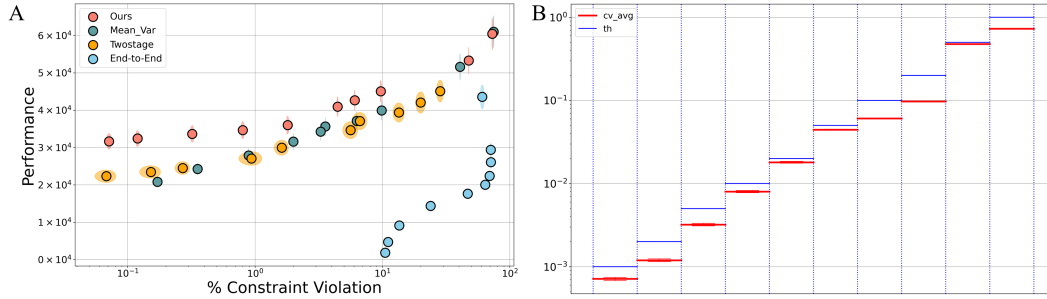


Figure 2: Production planning performance versus constraint violation. The x -axis shows the percentage of nonzero production cases despite actual demand below 30, and the y -axis represents the total revenue across 8,760 time steps. The proposed method achieves significantly higher revenue compared to baseline approaches, particularly at low constraint violation percentages.

5.2 Reinforcement learning in Safetygym

To demonstrate that our proposed framework can provide safety guarantees in reinforcement learning (RL), we apply it to standard RL methods and evaluate performance in the SafetyGym simulator Ray et al. [2019b]. In particular, we implement our framework in two SafetyGym environments: Safexp-PointGoal1-v0 and Safexp-Cargo1-v0, where the unknown state \mathbf{s} includes the agent speed and the exact location of the agent, goal, and unsafe regions, \mathbf{s}_{cr} is whether each discretized action candidate (explained later) is safe, and measurement \mathbf{y} is the output from LIDAR and IMU sensors. The objective is to compute action \mathbf{u} of the agent to reach the goal location without entering unsafe regions.

AI model: We integrate our method with standard RL approaches, proximal policy optimization (PPO) Schulman et al. [2017] and PPO-Lagrangian Jayant [2022]. These algorithms provide the mean and variance of the action distribution $\mathbf{o}_{ncr} = (\mu, \sigma)$, which we use to construct the recommended

action distribution as a normal distribution $\pi = \mathcal{N}(\mu, \sigma)$. Our approach discretizes the continuous action space so that $\mathcal{U} = \{\bar{\mathbf{u}}_1, \dots, \bar{\mathbf{u}}_{n_{ucd}}\}$ and evaluates safety for each discretized action candidate. Specifically, we use a safety classification model (size-reduced form of the original model) to yield $\mathbf{o}_{cr} = (\bar{o}_1, \dots, \bar{o}_{n_{ucd}})$ where $\bar{o}_i = 1$ if $\bar{\mathbf{u}}_i$ is unsafe and 0 if it is safe. We estimate collision probabilities for each discretized action candidate using the classification model, internal test data, and conservative testing.

Internal test data: We pretrain PPO agents for 10,000 epochs and use the resulting checkpoints to collect internal test cases through agent-environment interactions. Unlike supervised learning, where internal test cases can be directly selected from an existing labeled dataset, in RL we generate internal test cases through simulation. Each internal test case consists of observation \mathbf{y} , actions \mathbf{u} , and safety labels \mathbf{s}_{cr} , indicating whether the agent enters a hazardous region within 60 time steps.

Optimization: We sample the action among the discretized action candidates based on the following optimization problem:

$$\begin{aligned} \min_{\mathbf{u} \sim \pi^d} \quad & \bar{J}(\mathbf{u}) \\ \text{subject to} \quad & \log p^\xi(\mathbf{s}_{cr} = 1 | \mathbf{o}_{cr} = \mathbf{o}) \leq \log r_t, \end{aligned}$$

where π^d is π restricted to the discretized action candidate \mathcal{U} and default action $\hat{\mathbf{d}}$ (maximum braking). We use the log operation to handle extremely low thresholds, e.g., $r_t = 10^{-4}$. We let $\bar{J}(\hat{\mathbf{d}}) > 0$ and $\bar{J}(\bar{\mathbf{u}}_i) = 0$ for all other action candidates. This way, we apply the default action $\hat{\mathbf{d}}$ when all actions are hazardous. Given the classification output \mathbf{o} , the posterior probability $p^\xi(\mathbf{s}_{cr} = 1 | \mathbf{o}_{cr} = \mathbf{o})$ is computed by (8) using internal test data and conservative testing. We use $\xi = \frac{10^5}{n_t}$ for all cases.

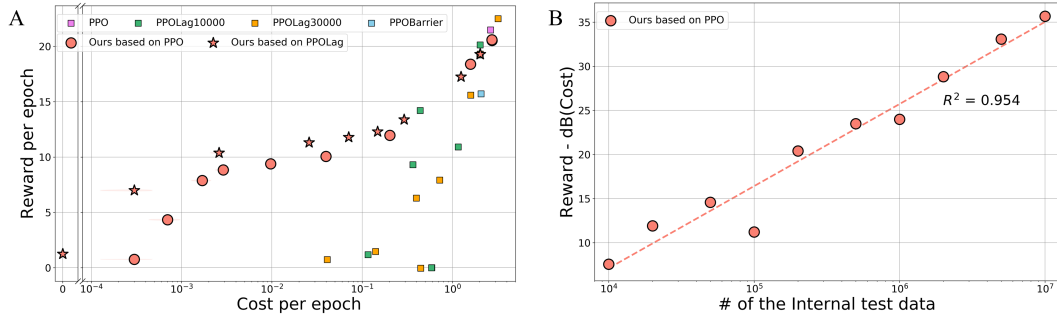


Figure 3: (A) RL safety versus performance. The x -axis is the average number of collisions per epoch, and the y -axis is the average reward per epoch. We use 10^7 internal test data in these experiments. For the baselines, we report PPO checkpoints trained for 10,000 epochs (violet), PPO-Barrier checkpoints trained for 10,000 epochs (blue), and several PPO-Lag checkpoints obtained by varying the cost limit from 0 to 2, trained for either 10,000 epochs (green) or 30,000 epochs (yellow). Our method achieves dramatically lower collision rates compared to the baselines, reaching below 10^{-5} while maintaining competitive performance. (B) RL scaling law. The x -axis shows the number of internal test data n_t , and the y -axis represents the reward minus decibel of the cost presented in the former plot. The proposed method shows a clear scaling law between the number of internal test data and the combined performance of reward maximization and cost minimization.

Results: Figure 3 illustrates the trade-off between safety and performance in our RL experiments. The x -axis (cost per epoch) indicates the average number of hazard encounters (each with a cost of 1) for each epoch (1,000 time steps). The y -axis shows the average reward for each epoch, where the agent receives a reward proportional to its progress toward the goal at each step and a reward of 1 upon reaching the goal. In this experiment, we use $r_t = 10^{-4}$ for training and 10 different values in $[10^{-5}, 1 + 10^{-5}]$ for validation. Our framework significantly outperforms all baseline methods in terms of safety, achieving collision rates below 10^{-5} with certain threshold settings – a safety level unattainable by other approaches – while maintaining competitive performance. This ultra-low collision rate represents a critical advancement for safety-critical applications like autonomous driving, where even extremely rare failures can have catastrophic consequences.

Figure ?? shows the clear scaling law between the number of internal test data and the combined performance of reward maximization and cost minimization. The x -axis shows the number of internal test data, while the y -axis presents the reward (y -axis value in the former plot) minus the decibel of cost (x -axis value in the former plot). This linear relation meets with the scaling law introduced in the former section.

5.3 Natural language generation

Large Language Models (LLMs) have been employed in various applications that are becoming key part of many people’s lifestyle, from commercial chatbots (e.g., GPT-4, Claude) to clinical decision-making Singhal et al. [2022] and educational support Wang et al. [2024]. As these systems become deeply embedded in society, their safety becomes paramount. For instance, chatbots and educational agents must avoid misinformation, discriminatory content, and unethical influences. LLMs face inherent safety challenges from potential learning and reproducing harmful content from their training data Su et al. [2024]. While instruction tuning methods have made progress in aligning LLMs with human preferences for both helpfulness Li et al. [2024] and harmlessness Ji et al. [2023], they lack mechanisms to probabilistically guarantee safety levels in deployment.

To address the challenge, we adapt our framework to guarantee arbitrary safety levels while maximizing helpful responses, providing a mathematically rigorous method for achieving probabilistic safety guarantees in LLM outputs and enabling practitioners to specify and maintain desired safety thresholds across different deployment contexts.

Our chance-constraint optimization framework integrates with any existing LLM alignment methods, including SFT Ouyang et al. [2022], PPO Schulman et al. [2017], Ouyang et al. [2022], DPO Rafailov et al. [2024], and PPO-lag Wu et al. [2023].

In this example, we fix the AI model, and thus denote it as π rather than $f(\mathbf{y}; \mathbf{w}_{ncr})$ since we do not train it, and serially connect it with the safety classification model $f(\mathbf{y}; \mathbf{w}_{cr})$. With a fixed π , the state is 16 answer candidates (\mathbf{s}_{ncr}) and whether they are safe (\mathbf{s}_{cr} : 16-dimensional binary vector). In this example, the answer candidates \mathbf{o}_{ncr} is equivalent \mathbf{s}_{ncr} in principle. They are obtained from π , and then concatenated with the input \mathbf{y} and get into the safety classification model.

Given a base model π fine-tuned using any alignment method, we add a rejection sampling layer using safety classification model trained with the proposed framework to ensure safety guarantees. To do so, we frame rejection sampling as a simple optimization problem as follows:

$$\arg \min_i 1 \tag{11}$$

$$\text{s.t. } \bar{c}(y_i; x) \geq 0 \tag{12}$$

where $y_i \sim \pi(\cdot|x)$ given prompt x and \bar{c} is the chance constraint given by the safety classification model.

Figure 4 shows that outputs generated using our method always satisfies the target safety threshold regardless of base generator model, while all baseline methods fails to satisfy safety threshold under 10

6 Discussion

In this paper, we propose a domain-agonistic framework that constructs a system that outputs safe and high performing action based on an AI model. We show the validity and the performance of our framework based on both theoretical construction and experiments in three distinct domains. Compared to existing methods, the point that our method internally evaluate the safety and provide tailored gradient to obtain safe and high performance action make our framework powerful to obtain much safer system. Provided that there are sufficiently many internal test data, our system can employ the tailored training gradient and large training epochs based on the theoretical guarantee given by the conservative testing. This allows extra training capacity regarding safety compared to existing methods that should run training with extra care to prevent overfitting.

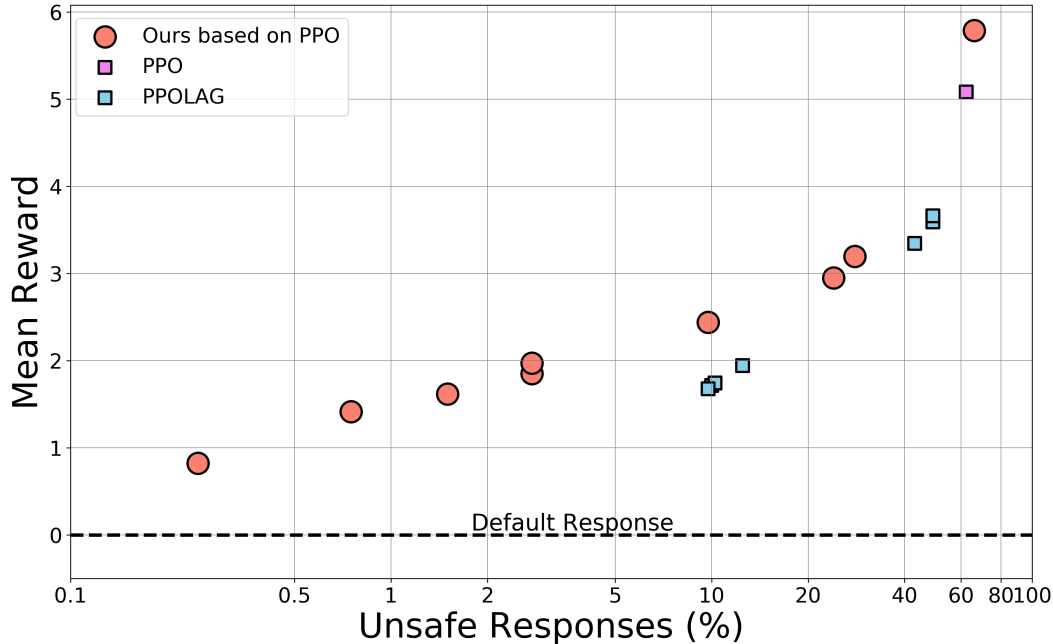


Figure 4: Natural language generation performance: x axis denotes percent of safe responses. y axis denotes average reward for 400 prompts. The proposed method obtains significantly safer responses.

In the experiments, through all domains for experiment, our framework achieve at least 3.7 times to order(s) of magnitude improvement for safety with similar or superior performance under lowest threshold cases. This results suggest that this framework has the potential to dramatically improve the safety of such domains.

Our framework provides a system that not only complies with user-defined safety constraints and thresholds, but also adapts to user preferences while maintaining operational transparency. Users can flexibly adjust constraints, thresholds, objective functions, and parameters to tailor the system to their specific needs. When users change these elements and retrain the system, it updates both AI model and safety classification model based on optimizing objectives under the specified constraints. Users can examine how the system interprets situations by monitoring the outputs of AI model and classification model, and how the system makes decisions by monitoring optimization input and output. Therefore, our approach achieves both customizability and transparency.

Based on the theoretical guarantee, performance, and its domain-agnostic manner, this framework can be a game changer for various safety-critical domains. Moreover, the customizability and transparency makes the framework a suitable method to enhance the alignment of AI in addition to the safety. Therefore, we expect this method to be a key milestone for safe and human-aligning deployment of AI and AI-related robotics. To maximize practical applicability, we provide an organized implementation suite of our framework that can integrate with any AI model across various applications, available for non-commercial use.

References

- Javier García and Fernando Fernández. A comprehensive survey on safe reinforcement learning. *Journal of Machine Learning Research*, 16(42):1437–1480, 2015. 2,100 citations (Google Scholar, April 2025).
- Marco Tulio Ribeiro, Sameer Singh, and Carlos Guestrin. “Why Should I Trust You?”: Explaining the predictions of any classifier. In *Proceedings of the 22nd ACM SIGKDD International Conference on Knowledge Discovery and Data Mining*, pages 1135–1144, 2016. doi: 10.1145/2939672.2939778.

- Ninareh Mehrabi, Fred Morstatter, Nripsuta Saxena, Kristina Lerman, and Aram Galstyan. A survey on bias and fairness in machine learning. *ACM Computing Surveys*, 54(6):1–35, 2021. doi: 10.1145/3457607.
- Volodymyr Mnih, Koray Kavukcuoglu, David Silver, Andrei A. Rusu, Joel Veness, Marc G. Belle-mare, Alex Graves, Martin Riedmiller, Andreas K. Fidjeland, Georg Ostrovski, Stig Petersen, Charles Beattie, Amir Sadik, Ioannis Antonoglou, Helen King, Dharshan Kumaran, Daan Wierstra, Shane Legg, and Demis Hassabis. Human-level control through deep reinforcement learning. *Nature*, 518(7540):529–533, February 2015. ISSN 1476-4687. doi: 10.1038/nature14236. URL <https://doi.org/10.1038/nature14236>.
- Dario Amodei, Chris Olah, Jacob Steinhardt, Paul Christiano, John Schulman, and Dan Mané. Concrete problems in AI safety. *arXiv preprint arXiv:1606.06565*, 2016. Over 3,000 citations (Google Scholar, April 2025).
- Ian J. Goodfellow, Jonathon Shlens, and Christian Szegedy. Explaining and harnessing adversarial examples. *International Conference on Learning Representations (ICLR)*, 2015.
- Guy Katz, Clark Barrett, David L. Dill, Kyle Julian, and Mykel J. Kochenderfer. Reluplex: An efficient SMT solver for verifying deep neural networks. In *Proceedings of the 29th International Conference on Computer Aided Verification (CAV)*, pages 97–117, 2017. doi: 10.1007/978-3-319-63387-9_5.
- Rüdiger Ehlers. Formal verification of piece-wise linear feed-forward neural networks. In *Proceedings of the 15th International Symposium on Automated Technology for Verification and Analysis (ATVA)*, volume 10482 of *Lecture Notes in Computer Science*, pages 269–286, 2017. 600 citations (Google Scholar, April 2025).
- Xin Huang, Marta Kwiatkowska, Sen Wang, and Min Wu. Safety verification of deep neural networks. In *Proceedings of the 29th International Conference on Computer Aided Verification (CAV)*, pages 3–29, 2017. 1,200 citations (Google Scholar, April 2025).
- Priya L. Donti, Brandon Amos, and J. Zico Kolter. Task-based end-to-end model learning in stochastic optimization. In *Advances in Neural Information Processing Systems (NeurIPS)*, pages 5484–5494, 2017.
- James Kotary, Ferdinando Fioretto, Pascal Van Hentenryck, and Bryan Wilder. End-to-end constrained optimization learning: A survey. In *Proceedings of the 30th International Joint Conference on Artificial Intelligence (IJCAI)*, pages 4475–4482, 2021.
- Brandon Amos and J. Zico Kolter. OptNet: Differentiable optimization as a layer in neural networks. In *Proceedings of the 34th International Conference on Machine Learning (ICML)*, volume 70 of *Proceedings of Machine Learning Research*, pages 136–145, 2017.
- Bryan Wilder, Bistra Dilikina, and Milind Tambe. Melding the data-decisions pipeline: Decision-focused learning for combinatorial optimization. In *Proceedings of the AAAI Conference on Artificial Intelligence*, volume 33, pages 1658–1665, 2019.
- Adam N. Elmachtoub and Paul Grigas. Smart “predict, then optimize”. *Management Science*, 68(1): 9–26, 2022.
- Aaron Ferber, Bryan Wilder, Bistra Dilikina, and Milind Tambe. MIPaaL: Mixed integer program as a layer. In *Proceedings of the AAAI Conference on Artificial Intelligence*, volume 34, pages 1504–1511, 2020.
- Aaron M. Ferber, Taoan Huang, Daochen Zha, Martin Schubert, Benoit Steiner, Bistra Dilikina, and Yuandong Tian. SurCo: Learning linear surrogates for combinatorial nonlinear optimization problems. In *Proceedings of the 40th International Conference on Machine Learning (ICML)*, volume 202 of *Proceedings of Machine Learning Research*, pages 10034–10052, 2023.
- Marin Vlastelica, Anselm Paulus, Vít Musil, Georg Martius, and Michal Rolínek. Differentiation of blackbox combinatorial solvers. In *International Conference on Learning Representations (ICLR)*, 2020.

- Joshua Achiam, David Held, Aviv Tamar, and Pieter Abbeel. Constrained policy optimization. In *International Conference on Machine Learning (ICML)*, 2017.
- Mohammad Alshiekh, Roderick Bloem, Ruediger Ehlers, et al. Safe reinforcement learning via shielding. In *AAAI Conference on Artificial Intelligence*, 2018.
- Alex Ray, Joshua Achiam, and Dario Amodei. Benchmarking safe exploration in deep reinforcement learning. Technical report, OpenAI, 2019a.
- Tobias Enders, James Harrison, and Maximilian Schiffer. Risk-sensitive soft actor-critic for robust deep reinforcement learning under distribution shifts. *arXiv:2402.09992*, 2024.
- Yiming Yao et al. Constraint-conditioned policy optimization for versatile safe reinforcement learning. In *NeurIPS*, 2023.
- Mr. Bayes and Mr. Price. An essay towards solving a problem in the doctrine of chances. by the late Rev. Mr. Bayes, F. R. S. Communicated by Mr. Price, in a letter to John Canton, A. M. F. R. S. *Philosophical Transactions*, 53:370–418, 1763. ISSN 02607085.
- Alex Ray, Joshua Achiam, and Dario Amodei. Benchmarking Safe Exploration in Deep Reinforcement Learning. 2019b.
- John Schulman, Filip Wolski, Prafulla Dhariwal, Alec Radford, and Oleg Klimov. Proximal policy optimization algorithms, 2017. URL <https://arxiv.org/abs/1707.06347>.
- Ashish Kumar Jayant. Ppo lagrangian pytorch, 2022. URL <https://github.com/akjayant/PPOLagrangianPyTorch>.
- Karan Singhal, Shekoofeh Azizi, Tao Tu, S. Sara Mahdavi, Jason Wei, Hyung Won Chung, Nathan Scales, Ajay Tanwani, Heather Cole-Lewis, Stephen Pfohl, Perry Payne, Martin Seneviratne, Paul Gamble, Chris Kelly, Nathaneal Scharli, Aakanksha Chowdhery, Philip Mansfield, Blaise Aguerre y Arcas, Dale Webster, Greg S. Corrado, Yossi Matias, Katherine Chou, Juraj Gottweis, Nenad Tomasev, Yun Liu, Alvin Rajkomar, Joelle Barral, Christopher Semturs, Alan Karthikesalingam, and Vivek Natarajan. Large Language Models Encode Clinical Knowledge, December 2022. URL <http://arxiv.org/abs/2212.13138>. arXiv:2212.13138 [cs].
- Shen Wang, Tianlong Xu, Hang Li, Chaoli Zhang, Joleen Liang, Jiliang Tang, Philip S. Yu, and Qingsong Wen. Large language models for education: A survey and outlook, 2024. URL <https://arxiv.org/abs/2403.18105>.
- Jingtong Su, Julia Kempe, and Karen Ullrich. Mission Impossible: A Statistical Perspective on Jail-breaking LLMs, August 2024. URL <http://arxiv.org/abs/2408.01420>. arXiv:2408.01420 [cs].
- Bolian Li, Yifan Wang, Ananth Grama, and Ruqi Zhang. Cascade Reward Sampling for Efficient Decoding-Time Alignment, June 2024. URL <http://arxiv.org/abs/2406.16306>. arXiv:2406.16306 [cs, stat].
- Jiaming Ji, Mickel Liu, Juntao Dai, Xuehai Pan, Chi Zhang, Ce Bian, Chi Zhang, Ruiyang Sun, Yizhou Wang, and Yaodong Yang. BeaverTails: Towards Improved Safety Alignment of LLM via a Human-Preference Dataset, July 2023. URL <http://arxiv.org/abs/2307.04657>. arXiv:2307.04657 [cs].
- Long Ouyang, Jeff Wu, Xu Jiang, Diogo Almeida, Carroll L. Wainwright, Pamela Mishkin, Chong Zhang, Sandhini Agarwal, Katarina Slama, Alex Ray, John Schulman, Jacob Hilton, Fraser Kelton, Luke Miller, Maddie Simens, Amanda Askell, Peter Welinder, Paul Christiano, Jan Leike, and Ryan Lowe. Training language models to follow instructions with human feedback, March 2022. URL <http://arxiv.org/abs/2203.02155>. arXiv:2203.02155 [cs].
- Rafael Rafailov, Archit Sharma, Eric Mitchell, Stefano Ermon, Christopher D. Manning, and Chelsea Finn. Direct preference optimization: Your language model is secretly a reward model, 2024. URL <https://arxiv.org/abs/2305.18290>.
- Tianhao Wu, Banghua Zhu, Ruoyu Zhang, Zhaojin Wen, Kannan Ramchandran, and Jiantao Jiao. Pairwise proximal policy optimization: Harnessing relative feedback for llm alignment, 2023. URL <https://arxiv.org/abs/2310.00212>.